© 2018. Published by The Company of Biologists Ltd | Journal of Experimental Biology (2018) 221, jeb171694. doi:10.1242/jeb.171694

RESEARCH ARTICLE

Gestational low-protein intake enhances whole-kidney miR-192 and miR-200 family expression and epithelial-to-mesenchymal transition in rat adult male offspring

Letícia B. Sene[1], Victor Hugo Gonçalves Rizzi[1], José A. R. Gontijo[2] and Patricia A. Boer[2,*]

ABSTRACT

Studies have shown that adult offspring of mothers fed a protein-restricted diet during pregnancy present a pronounced reduction of nephron number associated with decreased fractional urinary sodium excretion and arterial hypertension. Additionally, recent advances in our understanding of the molecular pathways that govern the association of gestational nutritional restriction, intrauterine growth retardation and inflammation with impaired nephrogenesis, nephron underdosing and kidney fibrosis point to the epithelial to mesenchymal transition (EMT) as a common factor. In the current study, protein and sodium urinary excretion rates were evaluated in rats, and immunohistochemistry and western blot techniques were used to characterize kidney structure changes in 16 week old male offspring of mothers fed a low-protein diet during pregnancy (LP group) compared with age-matched (NP) controls. We also verified the expression of miRNA, mRNA and protein markers of fibrosis and the EMT in whole kidney prepared from LP offspring. We found, surprisingly, that arterial hypertension and long-term hyperfiltration, manifest by proteinuria, were associated with increased renal miR-192 and miR-200 family expression in 16 week old LP relative to age-matched NP rats. Measurement of kidney fibrosis and EMT-related protein markers, by histochemistry and immunoblot techniques, showed a significant rise of TGF-β1 and type-I collagen content in glomeruli and tubulointerstitial areas, accompanied by enhanced fibronectin and ZEB1 and decreased E-cadherin immunoreactivity in 16 week old LP offspring. The results were partially confirmed by increased gene (mRNA) expression of collagen 1α1, collagen 1α2 and ZEB1 in LP whole kidneys compared with those of age-matched NP offspring. In view of the presumed functional overload in the remaining nephrons, we suggest that hypertension and proteinuria development following maternal protein restriction may be a preponderant factor for EMT and structural kidney changes in LP offspring. However, our study was not wholly able to establish the precise role of miRNAs in LP kidney disorders. Thus, further studies will be required to assess the contribution of the miR family to renal injury in a gestational protein-restricted model of fetal programming.

KEY WORDS: Fetal programming, Low-protein diet, Renal dysfunction, miRNA expression, Epithelial-to-mesenchymal transition

[1]Morphology Department, Bioscience Institute at São Paulo State University (UNESP), Botucatu, São Paulo 18618-290, Brazil. [2]Hydrossaline Metabolism and Fetal Programming Laboratory, School of Medicine at Campinas State University (UNICAMP), Campinas, São Paulo 13083-894, Brazil.

*Author for correspondence (boer@fcm.unicamp.br)

J.A.R.G., 0000-0002-4658-385X; P.A.B., 0000-0002-1196-2606

Received 6 October 2017; Accepted 13 March 2018

INTRODUCTION

Gestational development is highly sensitive to disturbances in the maternal environment. Thus, an adverse intrauterine environment may alter normal development, promoting adaptive growth restriction and lower birthweight. Also, the metabolic profile may be altered, increasing the risk of disease development in adulthood (Langley-Evans, 2006, 2009). The Developmental Origins of Health and Disease (DOHaD) concept defines those gestational conditions that determinate changes to optimize the phenotype for adaptation in the postnatal environment. This process is known as fetal programming, with a seminal impact to developmental biology (Langley-Evans, 2009; Barker, 2003).

Previous studies in our laboratory have demonstrated that gestational protein restriction is associated with renal morphological and physiological changes. Temporary protein restriction results in intrauterine growth retardation associated with impaired nephrogenesis and nephron underdosing (Mesquita et al., 2010a,b; Vaccari et al., 2015; Rizzi et al., 2017; Custódio et al., 2017). This abnormality is correlated with abnormal renal nerve activity, reduced nephron number and decreased glomerular filtration area in animals with a higher propensity for arterial hypertension, glomerulosclerosis and chronic renal failure (CKD). Thus, in this gestational programming animal model, we may suppose that the effective reduction of glomerular filtration area promotes hyperflow and increased ultrafiltration pressure as a trigger to progressive sclerosis of glomeruli associated with tubular function disorders (Mesquita et al., 2010a,b).

Epigenetic processes that include the control of gene expression by microRNAs orchestrate intrauterine development. MicroRNA (miRNA) is small non-coding RNA that post-transcriptionally modulates gene expression by binding to the 3′ UTR of target mRNAs (Kim et al., 2003; Bartel, 2009). Studies have demonstrated that miRNAs are involved in many biological processes, including gene regulation, cell differentiation and proliferation, and apoptosis (Shivdasani, 2006; Li et al., 2008).

The miR-200 family (including miR-200a, miR-200b, miR-200c, miR-141 and miR-429) and miR-192 are involved in the control of the epithelial-to-mesenchymal transition (EMT) (Gregory et al., 2008a; Wang et al., 2010). The EMT is an essential biological phenomenon that comprises a series of plastic epithelial states between the epithelial and mesenchymal states (Kalluri and Weinberg, 2009; Liu, 2004). During the EMT, the epithelial cells lose cell–cell contact, acquiring a mesenchymal phenotype (Thiery and Sleeman, 2006). The phenotypic changes are associated with alterations in transcription factor gene expression accompanied by decreased expression of epithelial markers and enhanced expression of mesenchymal markers, such as E-cadherin and fibronectin, respectively (Kalluri and Weinberg, 2009). The EMT plays a fundamental role in pathophysiological

Journal of Experimental Biology (2018) 221, jeb171694. doi:10.1242/jeb.171694

processes of the renal fibrosis, a final common pathway that leads to CKD (Liu, 2004).

Whatever the kidney pathological process, renal interstitial fibrosis is a common finding associated with severe kidney structure disorder and, consequently, functional impairment (Liu, 2011). Transforming growth factor beta (TGF-β) triggers the tubular EMT, and its expression is up-regulated in several types of chronic kidney disease (Huang et al., 2015). Conversely, miR-200f downregulates the kidney EMT expression induced by TGF-β1, via reduction of the translation of zinc finger E-box-binding homeobox1/2 transcription factors (ZEB1 and ZEB2).

Recently, in isolated glomeruli, we found that male adult offspring of mothers fed a protein-restricted diet during pregnancy show reduced miR-200f expression associated with enhanced TGF-β1 and ZEB2 expression, which is related to glomerular EMT and expression of glomerular fibrosis markers (Sene et al., 2013). The current study was performed to evaluate miR-192 and miR-200f expression as well as EMT occurrence in whole kidney tissue from adult offspring following gestational protein restriction. Surprisingly, here we found a distinct pattern of miRNA expression in entire kidney tissue when compared with isolated glomeruli from these programmed animals.

MATERIALS AND METHODS

Animals and experimental design

The experiments were conducted on female and male age-matched Wistar HanUnib sibling-mated rats (250–300 g) obtained from colonies maintained under specific pathogen-free conditions in the Multidisciplinary Center for Biological Investigation CEMIB/Unicamp, Campinas, Brazil. The environment and housing conformed to the requirements for managing health and well-being of the rats during the experimental procedure. The Institutional Ethics Committee (protocol CEUA/UNESP no. 292) approved the study design and experimental protocol, and the general guidelines established by the Brazilian College of Animal Experimentation were followed throughout the investigation. Immediately after weaning at 3 weeks of age, animals were placed under controlled temperature (25°C) and lighting conditions (07:00 h–19:00 h), with free access to tap water and standard rodent laboratory chow. We designated as day 1 of pregnancy the day in which a vaginal smear presented sperm. The dams were maintained on isocaloric rodent laboratory chow with standard (normal) protein content (NP; 17% protein) or low-protein content (LP; 6% protein) diet, *ad libitum* intake, throughout the entire pregnancy. All dams groups were returned to the NP diet intake immediately after delivery. Studies have demonstrated that gestational protein restriction is followed by low birthweight in rats, which leads to changes in blood pressure and glucose metabolism, and anxiety-like behaviors in male compared with female offspring (Ozaki et al., 2001; Gillette et al., 2017). The sex hormones contribute to a sexual phenotype dimorphism in the fetal programming model of adult disease by modulating regulatory pathways critical in the long-term control of neural, cardiovascular and metabolic functions. Thus, this study was conducted only in male rats to avoid interference from sex-related differences. Offspring birthweight was measured and referenced to that of the whole litter. Only one male offspring from each litter was used for each of immunoblotting, histology and immunohistochemistry, renal function test and measurement of blood pressure, proteinuria and gene expression studies. The offspring were maintained on standard rodent laboratory chow with standard protein content under controlled room temperature and lighting conditions (see above) and followed up to 16 weeks of age. Food consumption was monitored daily and normalized to body mass. Systolic arterial pressure was measured in conscious 16 week old offspring (NP n=9 and LP n=8) by an indirect tail-cuff method using an electrosphygmomanometer (IITC Life Science – BpMonWin Monitor v.1.33) combined with a pneumatic pulse transducer/amplifier. This indirect approach allowed repeated measurements with a close correlation (correlation coefficient=0.975) compared with direct intra-arterial recording. The mean of three consecutive readings represented the blood pressure. Body mass was recorded weekly. Twelve day old and 16 week old male offspring were anesthetized with ketamine and xylazine injected intraperitoneally and killed by cardiac puncture, and the kidneys were collected for real-time PCR, western blot, Sirius Red, renal function test and immunohistochemistry analyses.

Renal function test and measurement of proteinuria

The renal function tests were performed on the last day at 16 weeks of age in unanesthetized, unrestrained NP (n=10) and LP (n=11) male offspring. Creatinine clearance was obtained using standard methodology (Mesquita et al., 2010a,b; Vaccari et al., 2015; Rizzi et al., 2017; Custódio et al., 2017). Briefly, after an overnight fast, each animal received a tap water load by gavage (5% of body mass), followed by a second amount of the same volume 1 h later, and spontaneously voided urine was collected over a 120 min period into a graduated centrifuge tube and measured gravimetrically. At the end of the experiment, blood samples were drawn through the cardiac puncture in anesthetized rats (75 mg kg^{-1} body mass ketamine i.p. and 10 mg kg^{-1} body mass xylazine i.p.), and urine and plasma samples were collected for analysis. Plasma and urine sodium and potassium concentrations were measured by flame photometry (Micronal, B262, São Paulo, Brazil), while creatinine concentrations were determined spectrophotometrically (Instruments Laboratory, Genesys V, Daly City, CA, USA). Proteinuria was detected using the Sensiprot Kit (Labtest, Lagoa Santa, Brazil).

Total RNA extraction

RNA was extracted from the whole kidney (n=5 for each group from 5 different mothers) using Trizol reagent (Invitrogen), according to the instructions specified by the manufacturer. Total RNA quantity was determined by the absorbance at 260 nm using a nanoVue spectrophotometer (GE Healthcare, Pittsburgh, PA, USA), and RNA purity was assessed by the A_{260}/A_{280} and A_{260}/A_{230} ratios (acceptable when both were >1.8). RNA integrity was ensured by obtaining an RNA integrity number (RIN) >8 with an Agilent 2100 Bioanalyzer (Agilent Technologies, Waldbronn, Germany).

Reverse transcription of miRNA and mRNA

cDNA was synthesized using TaqMan® microRNA Reverse Transcription kit (Life Technologies, Carlsbad, CA, USA), combined with Stem-loop RT Primers (Life Technologies) and High Capacity RNA-to-cDNA Master Mix (Life Technologies), according to the manufacturer's guidelines. For miRNA, 3 µl (10 ng) total RNA was mixed with 3 µl specific primers, 100 mmol l^{-1} dNTPs, 50 µl MultiScribe™ Reverse Transcriptase, 10× RT Buffer and 20 µl RNase inhibitor, and made up to a final volume of 4.5 µl with H_2O. The conditions were 16°C for 2 min, 42°C for 1 min, 50°C for 1 s and 85°C for 5 min. For mRNA, 10 µl total RNA was mixed with 4 µl Master Mix, 2 µl specific primers and made up to a final volume of 20 µl with H_2O. The conditions were 25°C for 5 min, 42°C for 30 min and 85°C for 5 min.

Real-time quantitative PCR (miRNAs)

Each cDNA of the miR-200 family (miR-200a, miR-200b, miR-200c, miR-141 and miR-429) and miR-192 was quantified by

real-time quantitative PCR using ABI Prism 7900 Sequence Detection System (Life Technologies). For each reaction, we used 10 µl TaqMan® Universal PCR Master Mix, 2 µl TaqMan MicroRNA Assay Mix (Life Technologies) and 1.5 µl cDNA in a final reaction volume of 20 µl. The cycling conditions were 95°C for 10 min; 45 cycles of 95°C for 15 s and 60°C for 1 min.

Real-time quantitative PCR (mRNAs)

For analysis of the expression level of ZEB1, ZEB2, desmin, fibronectin, ZO-1, E-cadherin, TGF-β1, col 1α1 and col 1α2 genes in renal tissue, qPCR was carried out with SYBR Green Master Mix, using specific primers for each gene (Table 1). Reactions were set up in a total volume of 20 µl using 5 µl of cDNA (diluted 1:100), 10 µl SYBR green Master Mix (Life Technologies) and 2.5 µl of each specific primer (5 nmol l^{-1}), and performed in the ABI Prism 7300 real-time PCR system (Life Technologies). The cycling conditions were 95°C for 10 min; 45 cycles of 95°C for 15 s and 60°C for 1 min.

Analysis of gene expression

To analyze differential gene expression, the miRNA or mRNA levels obtained for each gene (Table 1) were compared between the LP group and the corresponding NP group. In the present study, the expression of several 'endogenous' genes was tested in an experimental LP model before these assays. We used those least subject to variation, and more stable to normalization (see Materials and Methods). miRNA expression was normalized to that of the snRNA U6 and snRNA U87 reference genes (accession no.: NR_004394 and AF272707, respectively); mRNA expression was normalized to that of the *GAPDH*, *β-actin* and *TBP* genes. Relative gene expression was evaluated using the comparative quantification method (Pfaffl, 2001). All relative quantifications were assessed using DataAssist software v3.0, using the ΔΔCT method. PCR efficiencies were calculated by linear regression from the increase in fluorescence in the exponential phase using the program LinRegPCR v 11.1 (Ruijter et al., 2009). Data are expressed as fold-change (mean ±s.d., n=5) relative to the age-matched control group. The level of significance was set at P<0.05 versus the control group and, mandatorily, 0.5>fold-change>1.5.

Immunoblotting

The cortical and medullary kidney tissues (n=5 for each group from 5 different mothers) were removed, frozen in liquid nitrogen and stored at −80°C. Afterwards, the tissue was minced coarsely and homogenized immediately in 10 volumes of solubilization buffer [10 ml l^{-1} Triton-X 100, 100 mmol l^{-1} Tris pH 7.4, 10 mmol l^{-1} sodium pyrophosphate, 100 mmol l^{-1} sodium fluoride, 10 mmol l^{-1} EDTA, 10 mmol l^{-1} sodium vanadate, 2 mmol l^{-1} phenylmethylsulfonyl fluoride (PSMF) and 0.1 mg ml^{-1} aprotinin at 4°C], using a Polytron PTA 20S generator (model PT 10/35, Brinkmann Instruments, Westbury, NY, USA) operated at maximum speed for 20 s. The tissue extracts were centrifuged at 11,000 rpm at 4°C for 40 min, and the supernatants were used as a sample. Protein quantification was performed using the Bradford method. The samples were dissolved in Laemmli buffer, heated in a boiling water bath for 5 min and separated by SDS-PAGE (Bio-Rad Laboratories, Hercules, CA, USA). Equal amounts of protein (100 µg) of each sample were loaded per well onto preformed 4–15% gradient gels (Bio-Rad Laboratories) for 1 h 30 min at 100 V. After electrophoretic separation, proteins were transferred to nitrocellulose membranes and then blocked with a TBS-T solution containing 5% non-fat dry milk at room temperature for 1 h. Nitrocellulose blots were then incubated at 4°C overnight with primary antibodies diluted in TBS-T or 1% BSA as follows: E-cadherin (ab53033, 1:200, Abcam, Cambridge, UK), desmin (ab15200, 1:200, Abcam), ZEB1 (sc-10572, 1:200, Santa Cruz Biotechnology, Dallas, TX, USA), ZEB2 (sc-48789, 1:200, Santa Cruz Biotechnology), TGF-β1 (sc-146, 1:100, Santa Cruz Biotechnology), and collagen 1 (sc-8788, 1:100, Santa Cruz Biotechnology). Immunoreactivity bands were detected using the enhanced chemiluminescence substrate kit (Pierce ECL Western Blotting Substrate, GE Healthcare), the images were obtained by CCD camera (G: BOX Chemi, Syngen®, Sacramento, CA, USA), and band intensities were quantified by optical densitometry (UN-SCAn-IT gel, Gel & Graph Digitizing Software v6.1). β-Actin or α-tubulin was used as an endogenous control.

Histology and immunohistochemistry (IHC)

Animals were deeply anesthetized with a mixture of ketamine (75 mg kg^{-1} body mass, i.p.) and xylazine (10 mg kg^{-1} body mass, i.p.) and the level of anesthesia was controlled by monitoring the corneal reflex. The rats were transcardially perfused with saline followed by 4% paraformaldehyde in 0.1 mol l^{-1} phosphate buffer, pH 7.4. After perfusion, the kidneys (n=5 for each group from 5 different mothers) were removed, weighed and placed in the same fixative for 2 h, followed by 70% alcohol until processed for paraffin inclusion. The paraffin blocks were cut into sections of 5 µm thickness. By Sirius Red staining, we estimated the density of collagen. We also assessed the density of TGF-β1, type I collagen and fibronectin in the 30 cortical and medullary fields of histological sections (n=5 for each group). Briefly, the boundaries of glomerular tuff, tubulointerstitial cortical and medullary profiles were manually traced using a computer mouse and the average of immunoreactivity density readings (excluding vessels and perivascular tissues) was determined. Images were captured with a photomicroscope and analyzed by Olympus cellSens Dimension software. No immunoreactivity was seen in control experiments in which primary antibodies were omitted. For IHC, paraffin sections were incubated overnight at 4°C with anti-collagen 1

Table 1. Primer sequences for qPCR

Gene	Forward	Reverse
ZEB1	5′-CATTTGATTGAGCACATGCG-3′	5′-AGCGGTGATTCATGTGTTGAG-3′
ZEB2	5′-CCCTTCTGCGACATAAATACGA-3′	5′-TGTGATTCATGTGCTGCGAGT-3′
Desmin	5′-GCGTGACAACCTGATAGACG-3′	5′-GTTGGATTTCCTCCTGTAGTTTG-3′
Fibronectin	5′-AGACCCCAGGCACCTATCAC-3′	5′-TGGCCGTTTCAGGAAGGTTG-3′
TGF-β1	5′-GGACTCTCCACCTGCAAGAC-3′	5′-GACTGGCGAGCCTTAGTTTG-3′
Col 1a2	5′-ACAAGGTGCTCGTGGTTTCC-3′	5′-GCACCAGGCTGTCCTTTCAA-3′
E-Cadherin	5′-ATGAGGTCGGTGCCCGTATT-3′	5′-CTCGTTGGTCTTGGGGTCTGT-3′
ZO-1	5′-GAGGCTTCAGAACGAGGCTATTT-3′	5′-CATGTCGGAGAGTAGAGGTTCGA-3′
Col 1a1	5′-ACCTGTGTGTTCCCCACTCA-3′	5′-CTTCTCCTTGGGGTTTGGGC-3′

Table 2. Offspring body birthweight from the entire litter, and offspring body and kidney mass from 12 day old and 16 week old LP versus age-matched NP offspring

Body/kidney mass	NP	LP	*P*
At birth			
Birthweight (g)	6±0.06 (*n*=32)	5±0.09 (*n*=35)	0.0001
12 days old			
Body mass	24±0.6 (*n*=19)	21±0.5 (*n*=18)	0.0017
Left kidney/body mass	0.007±0.0002 (*n*=12)	0.006±0.0001 (*n*=11)	0.009
Right kidney/body mass	0.007±0.0002 (*n*=12)	0.006±0.0001 (*n*=11)	0.01
16 weeks old			
Body mass	456±15 (*n*=7)	472±10 (*n*=7)	0.3927
Left kidney/body mass	0.003±0.00008 (*n*=6)	0.003±0.0001 (*n*=6)	0.21
Right kidney/body mass	0.005±0.0002 (*n*=7)	0.004±0.0001 (*n*=7)	0.057

LP, offspring of rats fed a protein-restricted diet during pregnancy; NP, offspring of rats fed a normal diet during pregnancy. Birthweight is body mass with reference to that of the entire litter. Only one offspring from each NP and LP litter was used for the 12 day and 16 week data. The results are expressed as means±s.d. Student's *t*-test.

(1:1000, Sigma-Aldrich, St Louis, MO, USA), anti-fibronectin (1:100 Santa Cruz Biotechnology), anti-TGF-β1 (1:100 Santa Cruz Biotechnology), anti-E-cadherin (1:200 Abcam) and anti-ZEB1 e 2 (1:200 Santa Cruz Biotechnology) primary antibodies. Secondary antibodies were used according to the primary antibody. Sections were revealed with 3,3′-diaminobenzidine tetrahydrochloride (DAB, Sigma-Aldrich), counterstained with Mayer's hematoxylin, dehydrated and mounted.

Data and statistical analysis

Data obtained from this study are expressed as the mean±s.d. Comparisons involving only two means within or between groups were carried out using Student's *t*-test. Statistical analysis was performed with GraphPad Prism 5.01 for Windows (1992-2007 GraphPad Software, Inc., La Jolla, CA, USA). The level of significance was set at $P<0.05$. Data and material are available from the Unesp Repository: https://repositorio.unesp.br/bitstream/handle/11449/88971/000709437.pdf?sequence=1 and http://catalogodeteses.capes.gov.br/catalogo-teses/#!/

RESULTS

Kidney and body mass

Gestational protein restriction did not significantly change the pregnant dams' body mass during gestation. Also, it did not affect the number of offspring (NP: 10±3 versus LP: 11±4; $P=0.2784$) or the proportion of male and female offspring ($P=0.3245$) per litter. The birthweight of LP male pups (body mass with reference to that of the entire litter; $n=35$) was significantly reduced compared with that of NP pups ($n=32$) (5.0±0.09 g versus 6.0±0.06 g; $P=0.0001$) (Table 2). The body mass of 12 day old LP pups (21±0.5 g, $n=18$) remained lower than that of age-matched NP pups (24±0.6 g, $n=19$) ($P=0.0017$) (Table 2). However, at 16 weeks of age, the body mass of LP and NP rats was similar ($P=0.3927$). Additionally, at 12 days after birth, both the left and right kidney mass of LP offspring was significantly reduced when compared with that of age-matched NP offspring; however, at 16 weeks, kidney mass was similar in NP and LP offspring groups (Table 2). As shown in Table 3, the tail systolic arterial pressure was significantly higher ($P=0.0001$) in 16 week old LP offspring (148.8±11.7 mmHg, $n=10$) relative to that of age-matched NP offspring (121.5±5.9 mmHg, $n=10$).

Renal function

The data for renal function in the 16 week old offspring of both (NP and LP) groups are summarized in Table 3. There were no significant differences between serum sodium, potassium, lithium and creatinine levels in NP rats compared with those of the LP group. Urinary flow rates (data not included) and glomerular filtration rate, estimated by creatinine clearance (CCr), did not significantly differ among the groups during the renal tubule sodium handling studies (Table 3). Fractional urinary sodium excretion ($FENa^+$) was significantly lower in the LP rats than in the age-matched NP group: LP 0.96±0.036% versus NP 1.44±0.26% ($P\leq0.05$). Urine from LP rats (45.92±19.6 mg day^{-1}, $n=10$, $P=0.03$) showed an elevated protein level when compared with that of age-matched NP rats (17.41±4.9 mg day^{-1}, $n=10$), as shown in Table 3.

Expression profile of miR-192 and miR-200 family

In 12 day old offspring, the renal expression of all studied miRNAs in LP rats was not altered compared with that found in NP rats (Fig. 1A). In contrast, in 16 week old LP animals, the renal tissue miR-192 ($P=0.008$, fold-change=1.55), miR-141 ($P=0.0001$, fold-change=1.59), miR-200c ($P=0.007$, fold-change=1.59) and miR-429 ($P=0.0007$, fold-change=1.63) was significantly upregulated when compared to that observed in age-matched NP. The expression of miR-200a/b was unchanged (Fig. 1B).

Gene expression

The gene (mRNA) expression of collagen 1α1 (col 1a1; $P=0.0001$, fold-change=1.53), collagen 1α2 (col 1a2; $P=0.0001$, fold-change=2.15) and ZEB1 ($P=0.0001$, fold-change=1.96) was significantly increased in whole kidneys from 16 week old LP rats

Table 3. Arterial blood pressure, creatinine clearance (CCr), fractional urinary sodium excretion ($FENa^+$) and proteinuria in 16 week old LP versus age-matched NP offspring

Groups	Blood pressure (mmHg)	CCr (ml min^{-1} 100 g^{-1} body mass)	$FENa^+$ (%)	Proteinuria (mg day^{-1})
NP	121.5±5.9	1.20±0.2	1.44±0.26	17.41±4.9
LP	148.8±11.7*	1.04±0.2	0.96±0.036*	45.92±19.6*

n=10 for each group. Only one offspring from each NP and LP litter was used. *n*=10 for each group.
Data are means±s.d. *$P\leq0.05$ versus LP (Student's *t*-test).

Journal of Experimental Biology (2018) 221, jeb171694. doi:10.1242/jeb.171694

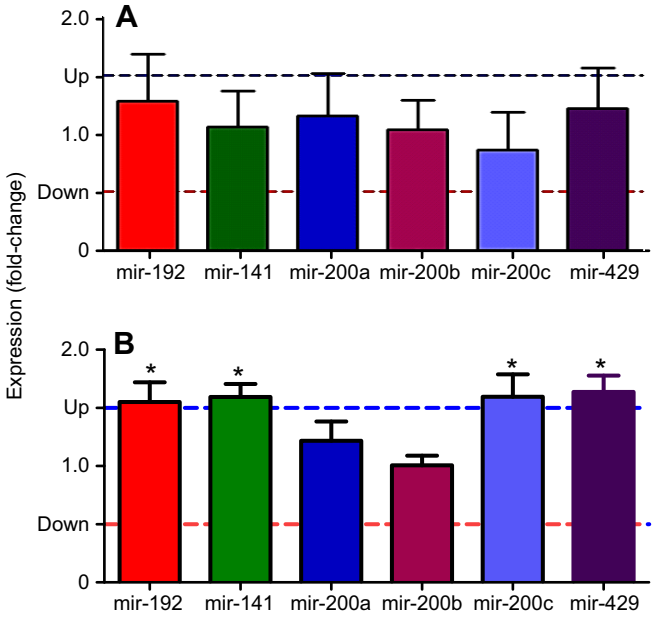

Fig. 1. miR-200 family and miR-192 expression profile. Data are the fold-change (mean±s.d., *n*=5) in expression in (A) 12 day old and (B) 16 week old offspring of rats fed a protein-restricted diet during pregnancy (LP) compared with those fed a normal diet (NP; age-matched controls). Expression of the snRNA U6 and snRNA U87 reference genes (accession no. NR_004394 and AF272707, respectively) was used for normalization of miRNA expression. Relative gene expression was evaluated using the comparative quantification method. miR-141 (P<0.0001), miR-200a (P=0.21), miR-200b (P=0.78), miR-200c (P=0.007), miR-429 (P=0.0007) and miR-192 (P=0.008). The level of significance (*) was set at P<0.05 versus NP group and 0.5>fold-change>1.5.

compared with that of age-matched NP offspring (Fig. 2). There was no difference in mRNA expression of desmin, E-cadherin, fibronectin, TGF-β1, ZEB2 and ZO-1 (Fig. 2).

Protein analysis

Analysis of fibrosis markers and EMT-related proteins showed a significant rise of the renal cortical and medullary TGF-β1 expression in 16 week old LP rats versus age-matched NP offspring (Fig. 3). The expression of extracellular matrix protein compounds was also enhanced in kidneys of 16 week old LP offspring. In the NP offspring, TGF-β1 expression was preferentially found in a basal portion of post-proximal nephron cells, whereas in LP offspring this protein was located in the extracellular matrix (Fig. 3). Picrosirius estimation analysis revealed significant enhancement of collagen content in the kidneys of 16 week old LP offspring versus the age-matched NP group (Fig. 4A–C). Cortical type I collagen immunoreactivity was found to be enhanced in adult LP offspring using both immunohistochemistry and western blot analysis (Fig. 4D–I). By western blot analysis, medullary type I collagen expression was significantly reduced in LP when compared both offspring groups (NP and LP) (Fig. 4K,L). However, no difference was observed by immunohistochemistry quantification (Fig. 4J). Also, fibronectin immunoreactivity was enhanced in the renal cortical and medullary areas of 16 week old LP offspring versus NP offspring (Fig. 5). Immunoreactivity to E-cadherin in the kidney was decreased (Fig. 6A,B) while that to ZEB1 was enhanced (Fig. 6D,E) in 16 week old LP rats when compared with age-matched NP offspring. The western blot semi-quantitative analyses confirmed a significant difference in the immunohistochemical studies (Fig. 6C,F). E-Cadherin expression (normalized to α-tubulin) by western blot in kidney medulla was unchanged (NP 100±41% versus LP 108±47%). Also, we did not find any difference in desmin and ZEB2 expression in LP compared with appropriate age-matched NP controls (Fig. 7).

DISCUSSION

More evidence is emerging that highlights the far-reaching consequences of maternal low-protein intake on kidney morphology and functional disorders. In the current study, confirming the findings of prior reports (Mesquita et al., 2010a,b; Vaccari et al., 2015), we demonstrated a reduction of 16% and 12% in LP offspring body mass at birth and after 12 days of life, respectively. At this time, the kidneys were also of lower mass (about 14%) in LP offspring when compared with age-matched NP offspring. However, we found no difference in body and kidney mass in the two groups at 16 weeks of age. Previously, we have shown, using the maternal protein and undernourished model, a reduced nephron number at 12 days and 12 weeks of age (about 27% and 35%, respectively) accompanied by enlarged remaining glomeruli in male LP offspring (Mesquita et al., 2010a; Vaccari et al., 2015). In the same studies, we also found a significant rise in arterial blood pressure in LP offspring associated with changes in renal nerve activity and in tubular sodium handling that lead to decreased urinary sodium excretion (Mesquita et al., 2010a,b; Vaccari et al., 2015; Custódio et al., 2017). A few years ago, Brenner et al. (1998) proposed that congenital reduction in nephron number makes some individuals susceptible to enhanced blood pressure and kidney injury (Brenner et al., 1998).

As mentioned above, a low number of nephrons at birth, the underdosing hypothesis, is linked to arterial hypertension and a greater propensity to progressive loss of renal function in adulthood

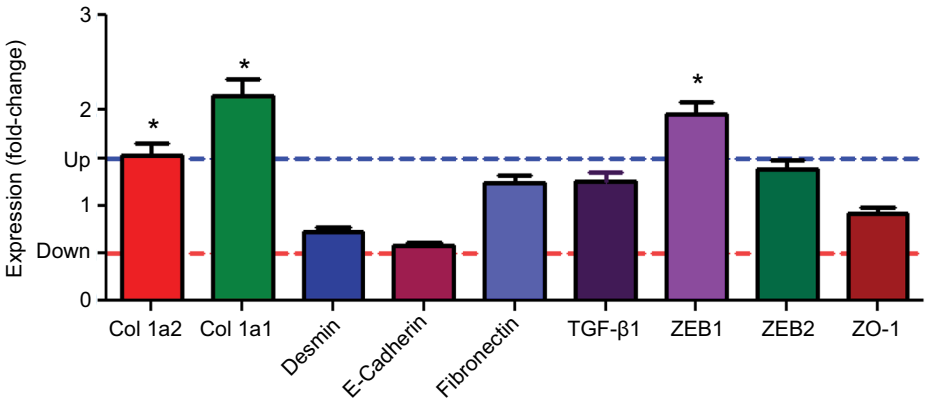

Fig. 2. Differential gene (mRNA) expression estimated by SYBR green qPCR from kidneys of 16 week old LP rats and age-matched NP offspring. Expression of each mRNA was normalized to that of GAPDH. Data are expressed as fold-change (mean±s.d., *n*=5) relative to the age-matched control group. col 1a2 (P<0.0001), col 1a1 (P<0.0001), desmin (P<0.0001), E-cadherin (P<0.0001), fibronectin (P=0.007), TGF-β1 (P=0.01), ZEB1 (P<0.0001), ZEB2 (P=0.0004) and ZO-1 (P=0.19). The level of significance (*) was set at P<0.05 versus NP group and 0.5>fold-change>1.5.

Journal of Experimental Biology (2018) 221, jeb171694. doi:10.1242/jeb.171694

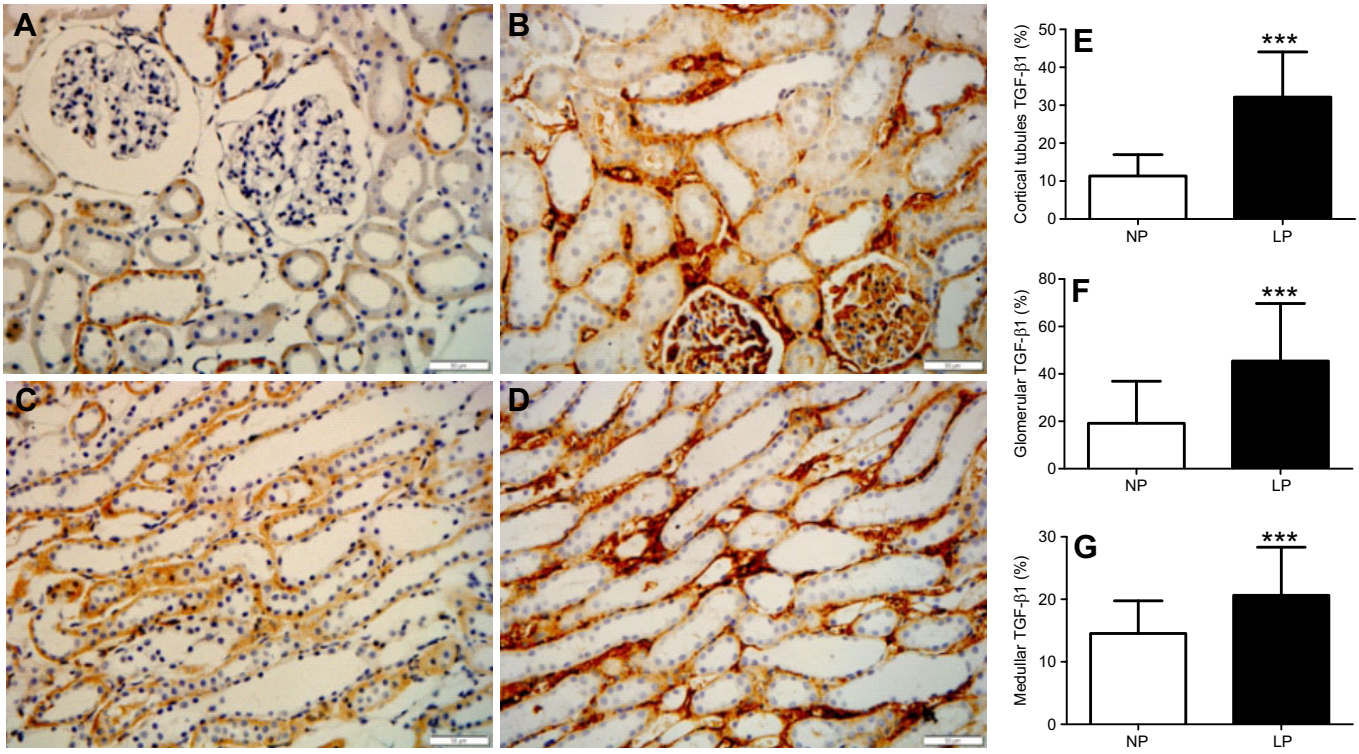

Fig. 3. TGF-β1 immunohistochemistry of renal tissue. (A–D) Images from 16 week old LP offspring (B,D) and age-matched NP offspring (A,C). (E–G) Quantification showed a significant rise of TGF-β1 in cortical (cortical tubules, E; glomerulus, F) and medullary (G) structures. Scale bars: 50 µm. Data are expressed as means±s.d. and the level of significance (*) was set at $P<0.05$ versus NP group; $n=5$ for each group.

(Mesquita et al., 2010a,b; Brenner et al., 1998). In the current study, maternal food-restricted offspring maintained a normal whole-kidney glomerular filtration rate, estimated by creatinine clearance, despite a decreased number of nephron units and a loss of efficiency in the filter barrier. Also, the present investigation demonstrated increased tubular sodium reabsorption accompanied by unchanged sodium-filtered load in LP rats. The precise mechanism of these phenomena remains unclear. However, our results sustain the hypothesis that fractional urinary sodium excretion and high blood pressure following maternal protein restriction could be associated with glomerular overflow and hyperfiltration of the remaining nephrons. These nephron hemodynamic changes could be the preponderant trigger for the development of altered glomerular ultrastructure, proteinuria and interstitial fibrosis processes in LP offspring. Thereby, the results of the current study using the maternal low-protein diet intake model support Brenner's theory, that the hyperfiltration in gestational protein-restricted offspring associated with low birthweight leads to glomerular hypertension, proteinuria and, in the future, to sustained renal function disorder and, consequently, fetal programming (Mesquita et al., 2010a,b; Sene et al., 2013; Brenner et al., 1998).

However, a great deal remains to be learned about nephron disorder in primary renal impairment of maternal protein-restricted offspring. It seems likely that glomerular and tubular structure change together, as initially suggested by Bricker et al. (1960) and Gottschalk (1971). Although in 16 week old LP rats, we cannot exclude the possibility that proteinuric glomerular disorder developed in response to an antecedent tubular or interstitial injury, recent reports have shown substantial evidence that, once established, the proteinuric glomerular injury may cause tubular dysfunction in the current experimental model (Mesquita et al., 2010a,b; Sene et al., 2013).

Podocytes are specialized epithelial lineage cells, incapable of postnatal replication, whose ontogenic differentiation process is finely orchestrated to produce specific characteristics such as foot processes (pedicels) interlinked by ultrathin slit diaphragms. Thus, podocyte injury is associated with podocyte pedicel effacement, reduction in the number and width of the interdigitating pattern of cell–cell connections and massive glomerular proteinuria (Mundel and Kriz, 1995), and is the potential starting-point for irreversible glomerular injury (Rizzi et al., 2017; Sene et al., 2013; Pippin et al., 1999; Fan et al., 2006; Villar-Martini et al., 2009). A prior study from our lab (Sene et al., 2013), using the same experimental model, confirmed that 16 week old LP offspring showed a striking podocyte structural alteration in parallel with proteinuria. In the same study, we also demonstrated enhanced desmin expression in isolated glomeruli associated with reduced expression of podocin and nephrin, indicating a decreased efficiency of the filtration barrier in LP rats when compared with age-matched control offspring. Nevertheless, the mechanism by which increased filtrated protein from diseased glomeruli into the tubular lumen causes cell injury has not been entirely clear.

Here, in a gestational low-protein model, we also focused on an ETM transdifferentiation process as a novel mechanism that promotes renal fibrosis. We investigated whether a known cause of renal fibrosis – TGF-β1 – acts through this pathway. By immunohistochemistry, we verified, in 16 week old LP offspring, a strikingly enhanced whole-kidney (cortex and medulla) expression of TGF-β1, fibronectin and type I collagen, intrinsically related to the fibrotic process. Nearly all LP offspring showed an increased expression (about 90%) of these proteins in the whole-kidney tissue. Simultaneously, by immunoblotting and immunohistochemistry of whole parenchyma, we found enhanced expression of ZEB1 accompanied by a fall in E-cadherin expression and followed by increased collagen deposition

Journal of Experimental Biology (2018) 221, jeb171694. doi:10.1242/jeb.171694

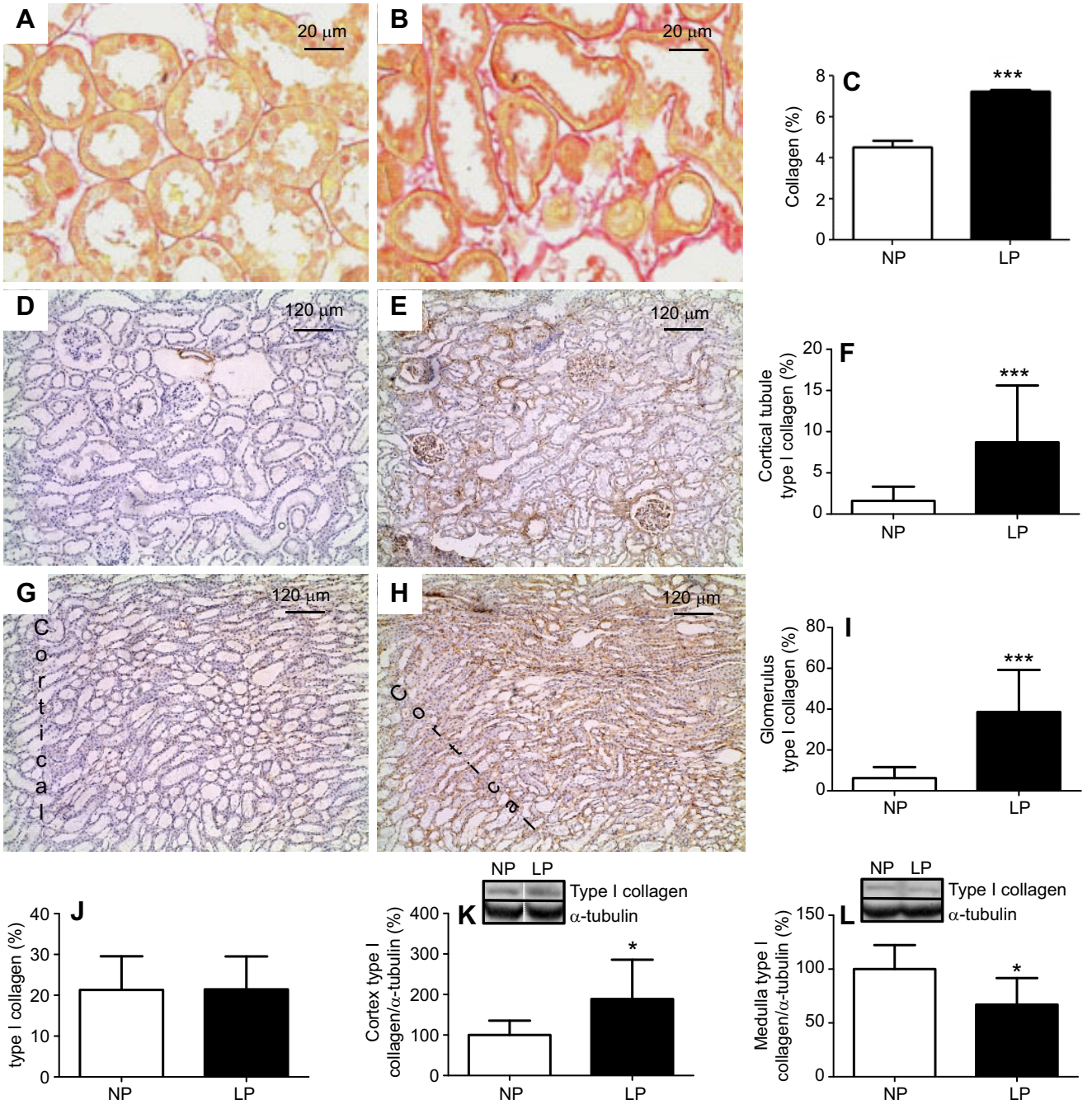

Fig. 4. Kidney collagen content. (A–C) Quantification of picrosirius-labeled area (C) in renal tissue from 16 week old NP (A) and LP (B) offspring. (D–J) Type 1 collagen immunohistochemistry in NP (D,G) and LP (E,H) kidneys. The quantification of reactivity showed a significant rise in cortical tissue of LP offspring (F,I). (K,L) Western blot quantification of cortical and medullary collagen (normalized to α-tubulin). Data are expressed as means±s.d. and the level of significance (*) was set at $P<0.05$ versus NP group; $n=5$ for each group.

in 16 week old LP compared with control NP group. We speculate whether the signaling receptors for specific bioactive proteins (such as TGF-β) on the tubular cell surface segments might be activated when increased amounts of those proteins are filtered or produced by damaged nephron cells. In this way, *in vitro* experiments have shown that activation of receptors for TGF-β1 stimulates tubular cell production of inflammatory mediators (Chung et al., 2010; Bracken et al., 2008; Xiong et al., 2012). In a culture of immortalized rodent kidney cells, Li et al. (2008) showed that after TGF-β1 expression, there was also a loss of epithelial markers, such as E-cadherin, and acquisition of mesenchymal markers, such as collagen I and fibronectin (Li et al., 2008).

The current study confirmed enhanced renal collagen 1α2 mRNA expression, which was accompanied by increased whole-kidney mRNA expression of ZEB1 and renal immunoreactivity to TGF-β1 and fibronectin in parallel with decreased expression of E-cadherin and no change of desmin mRNA expression in 16 week old LP offspring compared with age-matched NP rats. These results indicate that renal glomerular and tubular cells undergo phenotypic conversion, characterized by a loss of epithelium-specific markers

Journal of Experimental Biology (2018) 221, jeb171694. doi:10.1242/jeb.171694

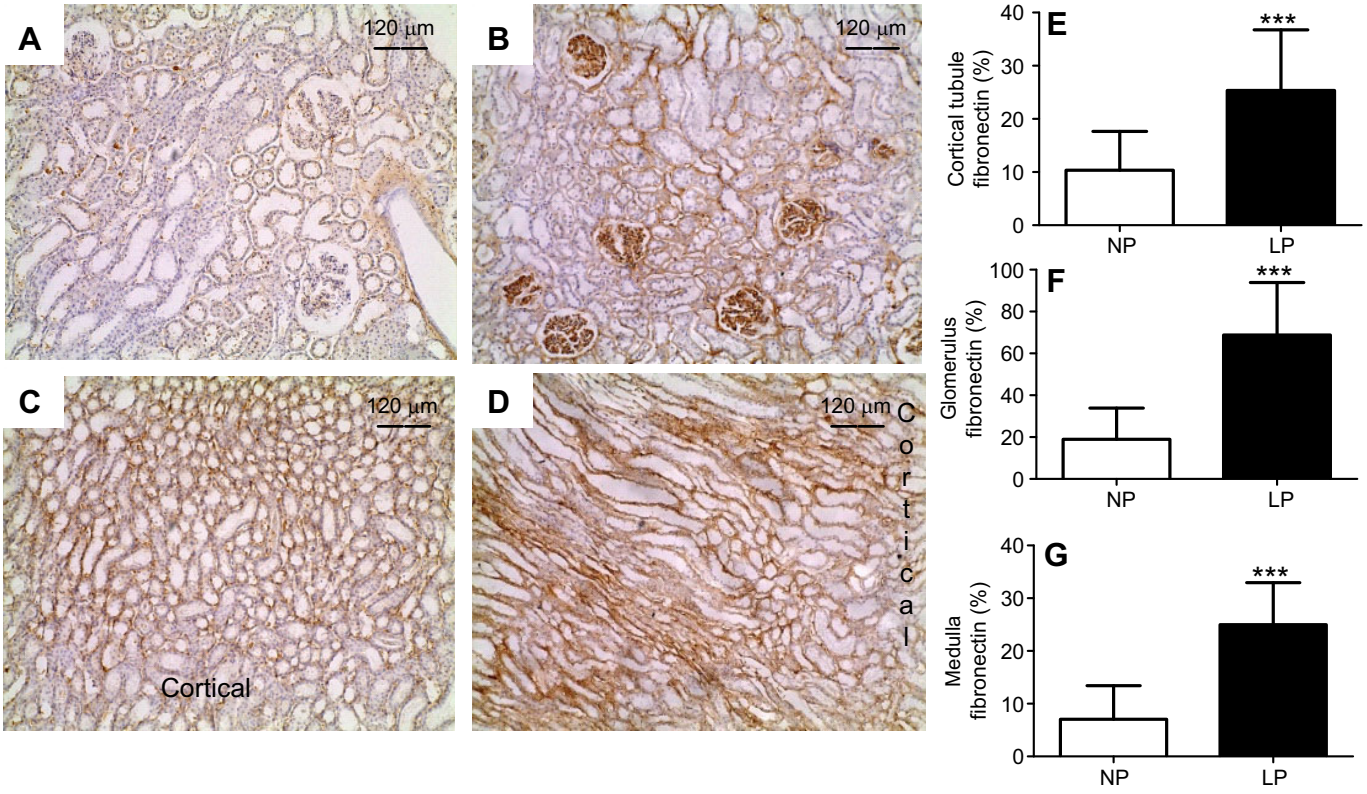

Fig. 5. Kidney fibronectin expression. Fibronectin immunohistochemistry from 16 week old LP (B,D) and age-matched NP (A,C) offspring. Quantification of immunoreactivity showed significantly enhanced expression in whole renal tissue of LP rats (E–G). Data are expressed as means±s.d. and the level of significance (*) was set at $P<0.05$ versus NP group; $n=5$ for each group.

and a gain of transitional features, a process reminiscent of EMT (Huang et al., 2015). In the current study as well as in our previous one (Sene et al., 2013), LP offspring kidneys showed enhanced expression of matrix markers (close to 80%). Results from studies in many kinds of cellular systems have demonstrated the upregulation of ZEB1 as an ordinary EMT marker triggered by overexpression of

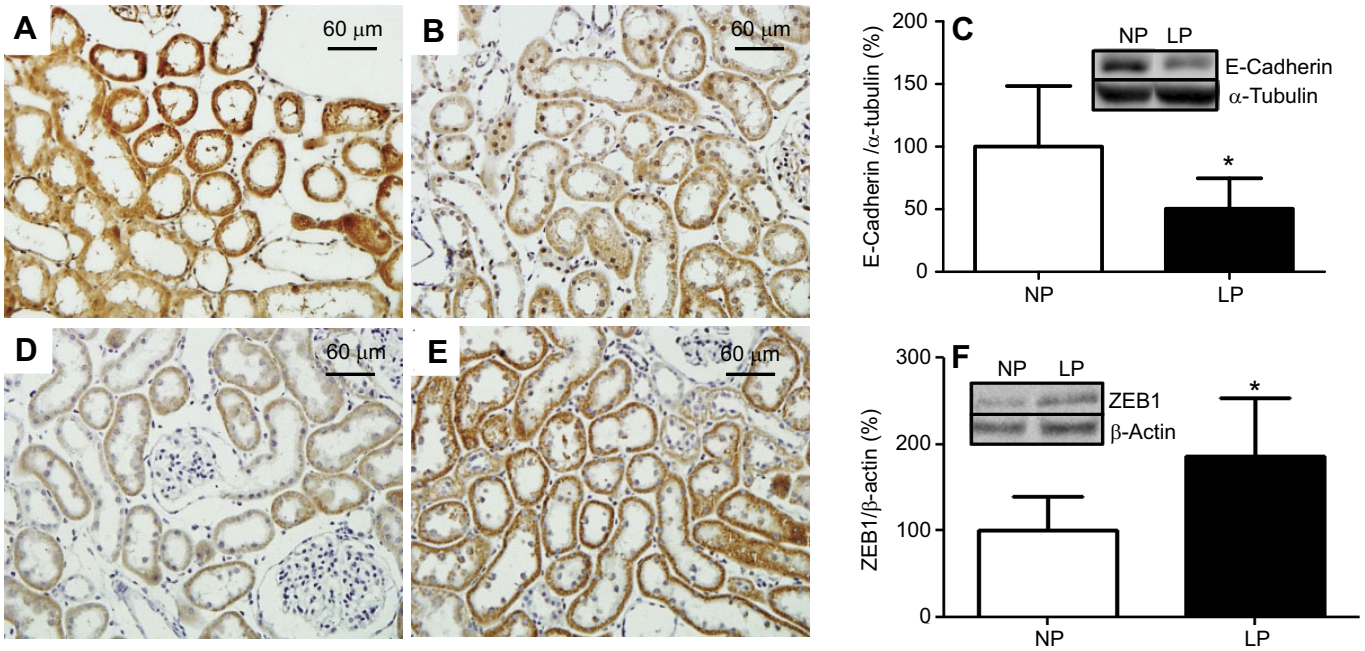

Fig. 6. Kidney E-cadherin and ZEB1 expression. E-Cadherin immunoreactivity (cortex) was decreased (A,B) while ZEB1 immunoreactivity was enhanced (D,E) in 16 week old LP rats when compared with age-matched NP offspring. The semi-quantitative western blot analyses confirm a significant difference in the immunohistochemical studies (C,F). Data are expressed as means±s.d. and the level of significance (*) was set at $P<0.05$ versus NP group; $n=5$ for each group.

Journal of Experimental Biology (2018) 221, jeb171694. doi:10.1242/jeb.171694

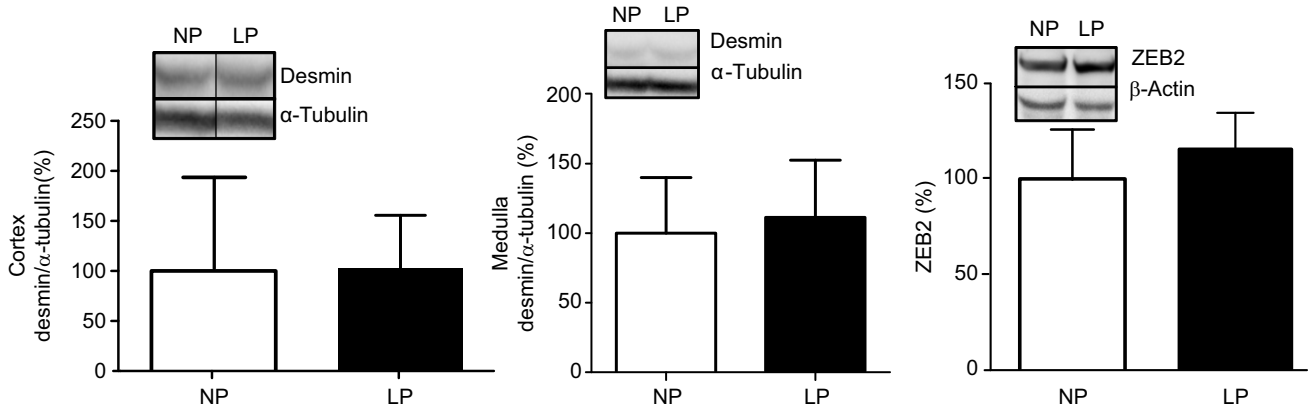

Fig. 7. Kidney desmin and ZEB2 expression. There was no difference in desmin and ZEB2 expression (assessed by western blot) in LP offspring relative to that of appropriate age-matched controls.

TGF-β1 (Kato et al., 2007; Christoffersen et al., 2007; Hurteau et al., 2007; Park et al., 2008; Burk et al., 2008; Korpal et al., 2008). Interestingly, here, ZEB1 was overexpressed in 16 week old LP offspring whole kidney, except in glomeruli, implicating it as a critical factor in the induction and maintenance of tubulointerstitial EMT. Thus, we may suppose that TGF-β1 triggers the tubular EMT and its expression is up-regulated in virtually every type of chronic kidney disease, including the LP programming model (Sene et al., 2013; Yang and Liu, 2001; Böttinger and Bitzer, 2002).

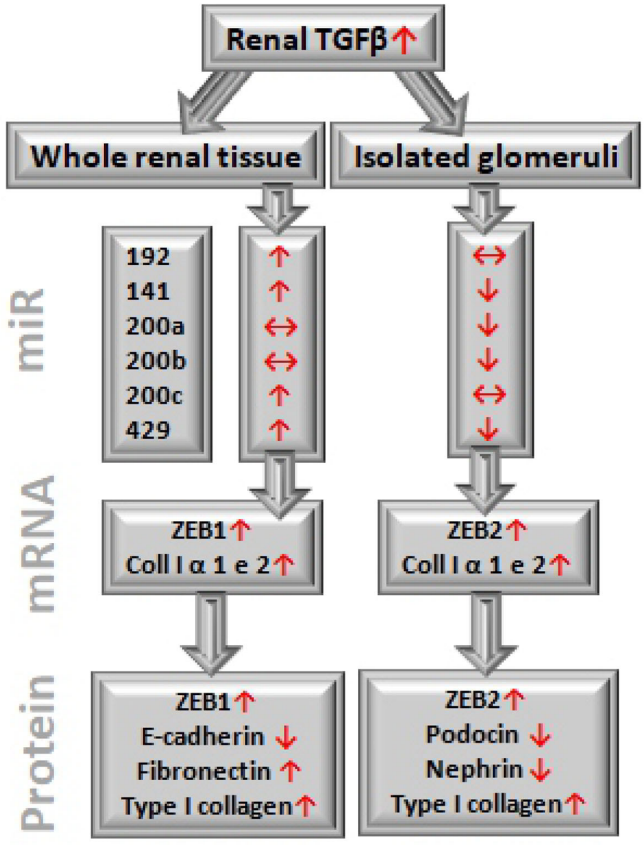

Fig. 8. Schematic representation of fetal programming consequences in isolated renal corpuscles versus whole kidney in 16 week old LP versus NP offspring.

miRNAs are small non-coding RNA of about 21 nucleotides that regulate gene expression in a post-transcriptional manner. Our study and prior studies have suggested that the TGF-β1 pathway promotes renal fibrosis by inducing renal miRNA expression (Li et al., 2008; Sene et al., 2013). As miRNAs have been proposed to play a pivotal role in a variety of kidney diseases, we investigated whether changes in the expression of the miR-200 family and miR-192 in whole kidney from 12 day old and 16 week old LP compared with age-matched NP offspring might also be involved in the renal pathogenesis of developmental abnormalities. At 12 days of life, there was no difference in the expression of these miRNAs, suggesting that their expression is not programmed during pregnancy and they are not expressed early, close to delivery. Conversely, this study showed that in 16 week old LP offspring, renal tissue miR-141 (160%), miR-200c (160%) and miR-429 (163%) were significantly upregulated when compared with levels observed in age-matched NP. In parallel, the mRNA for col 1a1/2 was also significantly increased (215% and 153%, respectively). These miRNA changes in 16 week old LP occurred in parallel to the enhanced expression of ZEB1 and TGF-β1, known inducers of EMT in epithelial cells (Li et al., 2008; Bracken et al., 2008; Xiong et al., 2012), and was associated with unchanged ZEB2 expression, an EMT-inducing transcriptional factor essential maintenance of the normal epithelial phenotype (Gregory et al., 2008a,b; Park et al., 2008; Korpal et al., 2008). Immunohistochemical analysis showed raised type 1 collagen immunoreactivity, which was more pronounced in glomeruli and the corticomedullary zone of kidneys. TGF-β1 protein expression was also enhanced in a similar pattern to that of type 1 collagen, but TGF-β1 mRNA expression was not altered.

Surprisingly, the present data do not support findings showing that renal glomerulus and tubule injury associated with fibrosis are related to downregulation of specific miRNAs (Sene et al., 2013; Ho et al., 2008; Shi et al., 2008; Wang et al., 2008; Li et al., 2015). Studies have demonstrated that miR-200 family members were downregulated in cells that had undergone EMT in response to TGF-β, and the expression of the miR-200 family alone was sufficient to prevent TGF-β-induced EMT (Gregory et al., 2008a,b). Also, in contrast to the current findings, the previous study from our laboratory (Sene et al., 2013) and that of Xiong et al. (2012) verified a downregulation of the miR-200 family induced by TGF-β1 in an isolated glomerulus preparation and kidney cell culture. Thus, although members of the miR-200 family have been implicated in inhibition of EMT in tubular cells, partially mediated through E-

cadherin restoration at the initiation of EMT (Gregory et al., 2008a,b), in the present study, we demonstrated a significant enhancement in the expression of mesenchymal protein markers, including fibronectin, collagen 1α1 and collagen 1α2. These results are supported by prior reports that have shown overexpression of miR-192 associated with renal fibrosis induced by TGF-β1 (Chung et al., 2010; Kato et al., 2007; Li et al., 2015; Wang et al., 2011). Also, Wang et al. (2010) demonstrated that intrarenal expression of miR-200a/b, miR-141, miR-429, miR-205 and miR-192 were increased in hypertensive nephrosclerosis and that the degree of upregulation was correlated with renal disease severity (Wang et al., 2010, 2011). Li et al. (2015) studied the miRNA profile of renal fibrosis and EMT in proximal tubular cells subjected to TGF-β1 treatment, and found induction of renal miR-21 and miR-433 expression. Wang et al. (2011) also reported differential transcription of miR-205 and miR-192 in IgA nephropathy, and these changes correlate with disease severity and progression. In contrast, Krupa et al. (2010) showed a reduction of miR-192 expression in the proximal tubular cells stimulated by TGF-β1. Although it is clear that the high levels of miR-192 are associated with functional and histopathological disorders, the report from Krupa et al. (2010) suggests that miRNA expression may have a dual role, such that elevation of miR-192 levels under certain conditions has a protective effect. Interestingly, these authors found that some miRNA (miR-633, miR-34a, miR-132, miR-155) were upregulated; conversely, others (miR-15a, miR-20b, miR-29c, miR-1303, miR-143 and miR-192-5p) were downregulated.

These contradictory findings highlight the complex nature of miRNA research, particularly in fetal programming models, in which many doubts persist. Notably, in our previous study using the same experimental model (Sene et al., 2013), we showed increased collagen deposition in isolated glomeruli, despite unchanged ZEB1 expression and, conversely, glomerular ZEB2 overexpression in 16 week old LP relative to NP offspring. These results led us to speculate that ZEB1/2 expression may have a specific function in different kidney structures. In comparison with our prior study (Sene et al., 2013), here we showed that the miRNA expression pattern was widely diverse in isolated glomeruli when compared with whole-kidney expression (see Fig. 8). The gene and protein data obtained in entire kidney studies do not necessarily reflect the expression presented in isolated nephron segments, which indicates the importance of analyzing isolated glomerulus and tubule structures. Taking into account that glomeruli, isolated nephron segments and interstitium are composed of a variety of cell types, we may suppose that the miRNA, mRNA and protein expression profile could be profoundly distinct in each nephron region. Kato et al. (2009) have considered the hypothesis that effects of renal miRNAs may be cell type specific, and miRNA signaling networks mediating the effects of TGF-β on different EMT cell types may be not the same. In the present study, we could not exclude the possibility of a post-transcriptional phenomenon in the gene pathway in response to reduced E-cadherin protein expression. Taking into account the above results, at least in part, we hypothesize that elevated expression of tubulointerstitial matrix markers in programmed rats indicates that kidney cells have adopted a mesenchymal phenotype, with a profound change in their morphology and function.

In the current study, we suggest that arterial hypertension and the long-term hyperfiltration process manifest by proteinuria were accompanied by increased whole-kidney mRNA expression of TGF-β1, ZEB1, type I collagen and fibronectin in parallel with decreased expression of E-cadherin in 16 week old LP offspring. Surprisingly, renal tissue miR-192, miR-141, miR-200c and miR-429 were significantly upregulated in LP offspring compared with age-matched NP rats. However, we were not entirely able to establish the exact role of miRNAs in LP kidney disorders, and this remains to be explored in this fertile research area. Thus, further studies will be required to assess the contribution of miRNA to renal injury in a gestational protein-restricted model of fetal programming.

Competing interests

The authors declare no competing or financial interests.

Author contributions

Conceptualization: J.A.G., P.A.B.; Methodology: J.A.G., L.B.S., V.G.R., P.A.B.; Validation: J.A.G., L.B.S., P.A.B.; Formal analysis: J.A.G., L.B.S.; Investigation: L.B.S., V.G.R., P.A.B.; Resources: J.A.G.; Data curation: J.A.G., L.B.S., V.G.R., P.A.B.; Writing - original draft: L.B.S.; Writing - review & editing: J.A.G., P.A.B.; Visualization: J.A.G.; Supervision: J.A.G., P.A.B.; Project administration: J.A.G., P.A.B.; Funding acquisition: J.A.G.

Funding

This work was supported by Fundação de Amparo à Pesquisa do Estado de São Paulo (#09/54141-9 and #13/12486-5), Conselho Nacional de Desenvolvimento Científico e Tecnológico (CNPq) and Coordenação de Aperfeiçoamento de Pessoal de Nível Superior (CAPES).

Data availability

Data and material are available from the Unesp Repository: https://repositorio.unesp.br/bitstream/handle/11449/88971/000709437.pdf?sequence=1 and http://catalogodeteses.capes.gov.br/catalogo-teses/#!/

References

Barker, D. (2003). The midwife, the coincidence, and the hypothesis. *BMJ* **327**, 1428-1430.

Bartel, D. P. (2009). MicroRNAs: target recognition and regulatory functions. *Cell* **136**, 215-233.

Böttinger, E. P. and Bitzer, M. (2002). TGF-beta signaling in renal disease. *J. Am. Soc. Nephrol.* **13**, 2600-2610.

Bracken, C. P., Gregory, P. A., Kolesnikoff, N., Bert, A. G., Wang, J., Shannon, M. F. and Goodall, G. J. (2008). A double-negative feedback loop between ZEB1-SIP1 and the microRNA-200 family regulates epithelial-mesenchymal transition. *Cancer Res.* **68**, 7846-7854.

Brenner, B. M., Garcia, D. L. and Anderson, S. (1998). Glomeruli and blood pressure: less of one, more the other? *Am. J. Hypertens.* **1**, 335-347.

Bricker, N. S., Morrin, P. A. F. and Kime, S. W.Jr. (1960). The pathologic physiology of chronic Bright's disease. An exposition of the "intact nephron hypothesis". *Am. J. Med.* **28**, 77-98.

Burk, U., Schubert, J., Wellner, U., Schmalhofer, O., Vincan, E., Spaderna, S. and Brabletz, T. (2008). A reciprocal repression between zeb1 and members of the mir-200 family promotes EMT and invasion in cancer cells. *EMBO Rep.* **9**, 582-589.

Christoffersen, N. R., Silahtaroglu, A., Orom, U. A., Kauppinen, S. and Lund, A. H. (2007). miR-200b mediates post-transcriptional repression of ZFHX1B. *RNA* **13**, 1172-1178.

Chung, A. C. K., Huang, X. R., Meng, X. and Lan, H. Y. (2010). miR-192 Mediates TGF-β/Smad3-driven renal fibrosis. *J. Am. Soc. Nephrol.* **21**, 1317-1325.

Custódio, A. H., de Lima, M. C., Vaccari, B., Boer, P. A. and Gontijo, J. A. R. (2017). Renal sodium handling and blood pressure changes in gestational protein-restricted offspring: role of renal nerves and ganglia neurokinin expression. *PLoS ONE* **12**, e0179499.

Fan, Q., Xing, Y., Ding, J., Guan, N. and Zhang, J. (2006). The relationship among nephrin, podocin, CD2AP, and alpha-actinin might not be a true 'interaction' in podocyte. *Kidney Int.* **69**, 1207-1215.

Gillette, R., Reilly, M. P., Topper, V. Y., Thompson, L. M., Crews, D. and Gore, A. C. (2017). Anxiety-like behaviors in adulthood are altered in male but not female rats exposed to low dosages of polychlorinated biphenyls in utero. *Hormone Behav.* **87**, 8-15.

Gottschalk, C. W. (1971). Function of the chronically diseased kidney. The adaptive nephron. *Circ. Res.* **28** Suppl. 2, 1-13.

Gregory, P. A., Bert, A. G., Paterson, E. L., Barry, S. C., Tsykin, A., Farshid, G., Vadas, M. A., Khew-Goodall, Y. and Goodall, G. J. (2008a). The mir-200 family and mir-205 regulate epithelial to mesenchymal transition by targeting zeb1 and sip1. *Nat. Cell Biol.* **10**, 593-601.

Gregory, P. A., Bracken, C. P., Bert, A. G. and Goodall, G. J. (2008b). MicroRNAs as regulators of epithelial-mesenchymal transition. *Cell Cycle* **7**, 3112-3117.

Ho, J., Ng, K. H., Rosen, S., Dostal, A., Gregory, R. I. and Kreidberg, J. A. (2008). Podocyte-specific loss of functional microRNAs leads to rapid glomerular and tubular injury. *J. Am. Soc. Nephrol.* **19**, 2069-2075.

Huang, Y., Tong, J., He, F., Yu, X., Fan, L., Hu, J., Tan, J. and Chen, Z. (2015). miR-141 regulates TGF-β1-induced epithelial-mesenchymal transition through repression of HIPK2 expression in renal tubular epithelial cells. *Int. J. Mol. Med.* **35**, 311-318.

Hurteau, G. J., Carlson, J. A., Spivack, S. D. and Brock, G. J. (2007). Overexpression of the microRNA hsa-miR-200c leads to reduced expression of transcription factor 8 and increased expression of E-cadherin. *Cancer Res.* **67**, 7972-7976.

Kalluri, R. and Weinberg, R. A. (2009). The basics of epithelial-mesenchymal transition. *J. Clin. Invest.* **119**, 1420-1428.

Kato, M., Zhang, J., Wang, M., Lanting, L., Yuan, H., Rossi, J. J. and Natarajan, R. (2007). MicroRNA-192 in diabetic kidney glomeruli and its function in TGF-beta-induced collagen expression via inhibition of E-box repressors. *Proc. Natl. Acad. Sci. USA* **104**, 3432-3437.

Kato, M., Arce, L. and Natarajan, R. (2009). MicroRNAs and their role in progressive kidney diseases. *Clin. J. Am. Soc. Nephrol.* **4**, 1255-1266.

Kim, J. H., Kim, B. K., Moon, K. C., Hong, H. K. and Lee, H. S. (2003). Activation of the TGF-β/Smad signaling pathway in focal segmental glomerulosclerosis. *Kidney Int.* **64**, 1715-1721.

Korpal, M., Lee, E. S., Hu, G. and Kang, Y. (2008). The miR-200 family inhibits epithelial-mesenchymal transition and cancer cell migration by direct targeting of E-cadherin transcriptional repressors ZEB1 and ZEB2. *J. Biol. Chem.* **283**, 14910-14914.

Krupa, A., Jenkins, R., Luo, D. D., Lewis, A., Phillips, A. and Fraser, D. (2010). Loss of MicroRNA-192 promotes fibrogenesis in diabetic nephropathy. *J. Am. Soc. Nephrol.* **21**, 438-447.

Langley-Evans, S. C. (2006). Developmental programming of health and disease. *Proc. Nutr. Soc.* **65**, 97-105.

Langley-Evans, S. C. (2009). Nutritional programming of disease: unravelling the mechanism. *J. Anat.* **215**, 36-51.

Li, Y., Kang, Y. S., Dai, C., Kiss, L. P., Wen, X. and Liu, Y. (2008). Epithelial-to-mesenchymal transition is a potential pathway leading to podocyte dysfunction and proteinuria. *Am. J. Pathol.* **172**, 299-308.

Li, Y., An, H., Pang, J., Huang, L., Li, J. and Liu, L. (2015). MicroRNA profiling identifies miR-192-5p as a regulator of EMT in tubular epithelial cells. *Int. J. Clin. Exp. Med.* **8**, 20610-20616.

Liu, Y. (2004). Epithelial to mesenchymal transition in renal fibrogenesis: pathologic significance, molecular mechanism, and therapeutic intervention. *J. Am. Soc. Nephrol.* **15**, 1-12.

Liu, Y. (2011). Cellular and molecular mechanisms of renal fibrosis. *Nat. Rev. Nephrol.* **7**, 684-696.

Mesquita, F. F., Gontijo, J. A. R. and Boer, P. A. (2010a). Expression of renin-angiotensin system signalling compounds in maternal protein-restricted rats: effect on renal sodium excretion and blood pressure. *Nephrol. Dial. Transplant.* **25**, 380-388.

Mesquita, F. F., Gontijo, J. A. R. and Boer, P. A. (2010b). Maternal undernutrition and the offspring kidney: from fetal to adult life. *Braz. J. Med. Biol. Res.* **43**, 1010-1018.

Mundel, P. and Kriz, W. (1995). Structure and function of podocytes: an update. *Anat. Embryol.* **192**, 385-397.

Ozaki, T., Nishina, H., Hanson, M. A. and Poston, L. (2001). Dietary restriction in pregnant rats causes gender-related hypertension and vascular dysfunction in offspring. *J. Physiol.* **530**, 141-152.

Park, S.-M., Gaur, A. B., Lengyel, E. and Peter, M. E. (2008). The miR-200 family determines the epithelial phenotype of cancer cells by targeting the E-cadherin repressors ZEB1 and ZEB2. *Genes Dev.* **22**, 894-907.

Pfaffl, M. W. (2001). A new mathematical model for relative quantification in real-time RT-PCR. *Nucleic Acids Res.* **29**, e45.

Pippin, J. W., Brinkkoetter, P. T., Cormack-Aboud, F. C., Durvasula, R. V., Hauser, P. V., Kowalewska, J., Krofft, R. D., Logar, C. M., Marshall, C. B., Ohse, T. et al. (1999). Inducible rodent models of acquired podocyte diseases. *Am. J. Physiol. Renal. Physiol.* **296**, F213-F229.

Rizzi, V. H. G., Sene, L. D., Fernandez, C. D. B., Gontijo, J. A. R. Boer, P. A. (2017). Impact of long-term high-fat diet intake gestational protein-restricted offspring on kidney morphology and function. *J. Dev. Orig. Health Dis.* **8**, 89-100.

Ruijter, J. M., Ramakers, C., Hoogaars, W. M. H., Karlen, Y., Bakker, O., van den Hoff, M. J. B. and Moorman, A. F. M. (2009). Amplification efficiency: linking baseline and bias in the analysis of quantitative PCR data. *Nucleic Acids Res.* **37**, e45.

Sene, L. B., Mesquita, F. F., de Moraes, L. N., Santos, D. C., Carvalho, R., Gontijo, J. A. R. and Boer, P. A. (2013). Involvement of renal corpuscle microRNA expression on epithelial-to-mesenchymal transition in maternal low protein diet in adult programmed rats. *PLoS ONE* **8**, e71310.

Shi, S., Yu, L., Chiu, C., Sun, Y., Chen, J., Khitrov, G., Merkenschlager, M., Holzman, L. B., Zhang, W., Mundel, P. et al. (2008). Podocyte-selective deletion of dicer induces proteinuria and glomerulosclerosis. *J. Am. Soc. Nephrol.* **19**, 2159-2169.

Shivdasani, R. A. (2006). MicroRNAs: regulators of gene expression and cell differentiation. *Blood* **108**, 3646-3653.

Thiery, J. P. and Sleeman, J. P. (2006). Complex networks orchestrate epithelial-mesenchymal transitions. *Nat. Rev. Mol. Cell Biol.* **7**, 131-142.

Vaccari, B., Mesquita, F. F., Gontijo, J. A. R. and Boer, P. A. (2015). Fetal kidney programming by severe food restriction: effects on structure, hormonal receptor expression and urinary sodium excretion in rats. *J. Renin Angiotensin Aldosterone Syst.* **16**, 33-46.

Villar-Martini, V. C., Carvalho, J. J., Neves, M. F., Aguila, M. B. and Mandarin-De-Lacerda, C. A. (2009). Hypertension and kidney alterations in rat offspring from low protein pregnancies. *J. Hypertens. Suppl.* **27**, S47-S51.

Wang, Q., Wang, Y., Minto, A. W., Wang, J., Shi, Q., Li, X. and Quigg, R. J. (2008). MicroRNA-377 is up-regulated and can lead to increased fibronectin production in diabetic nephropathy. *FASEB J.* **22**, 4126-4135

Wang, B., Herman-Edelstein, M., Koh, P., Burns, W., Jandeleit-Dahm, K., Watson, A., Saleem, M., Goodall, G. J., Twigg, S. M., Cooper, M. E. et al. (2010). E-cadherin expression is regulated by miR-192/215 by a mechanism that is independent of the profibrotic effects of transforming growth factor-β. *Diabetes* **59**, 1794-1802.

Wang, B., Koh, P., Winbanks, C., Coughlan, M. T., McClelland, A., Watson, A., Jandeleit-Dahm, K., Burns, W. C., Thomas, M. C., Cooper, M. E. et al. (2011). miR-200a prevents renal fibrogenesis through repression of TGF-{beta}2 expression. *Diabetes* **60**, 280-287.

Xiong, M., Jiang, L., Zhou, Y., Qiu, W., Fang, L., Tan, R., Wen, P. and Yang, J. (2012). The miR-200 family regulates TGF-β1-induced renal tubular epithelial to mesenchymal transition through Smad pathway by targeting ZEB1 and ZEB2 expression. *Am. J. Physiol. Renal. Physiol.* **302**, F369-F379.

Yang, J. and Liu, Y. (2001). Dissection of key events in tubular epithelial to myofibroblast transition and its implications in renal interstitial fibrosis. *Am. J. Pathol.* **159**, 1465-1475.